

SUPPLEMENTARY INFORMATION

Self-healing and super-elastomeric PolyMEA-co-SMA nanocomposites crosslinked by clay platelets

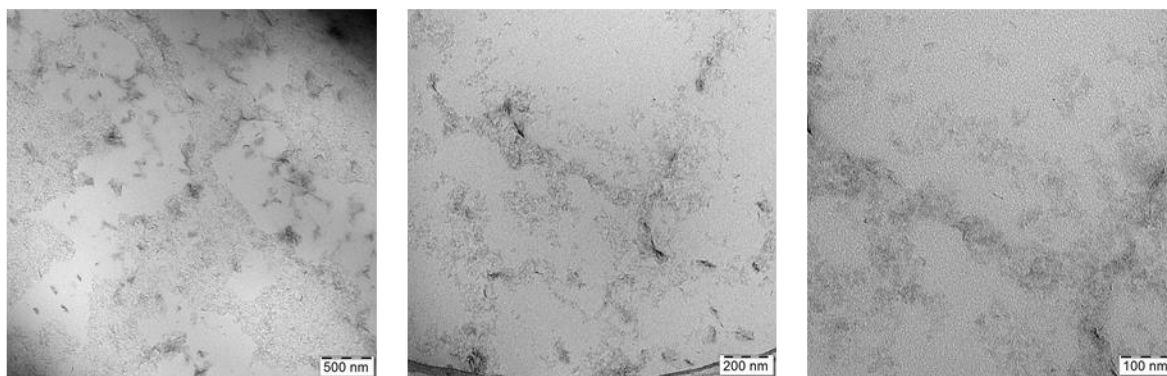
Beata Strachota¹, Adam Strachota^{1*}, Katarzyna Byś¹, Ewa Pavlova¹, Jiří Hodan¹,
Beata Mossety-Leszczak²

¹ *Institute of Macromolecular Chemistry, Czech Academy of Sciences
Heyrovskeho nam. 2, CZ-162 00 Praha, Czech Republic*

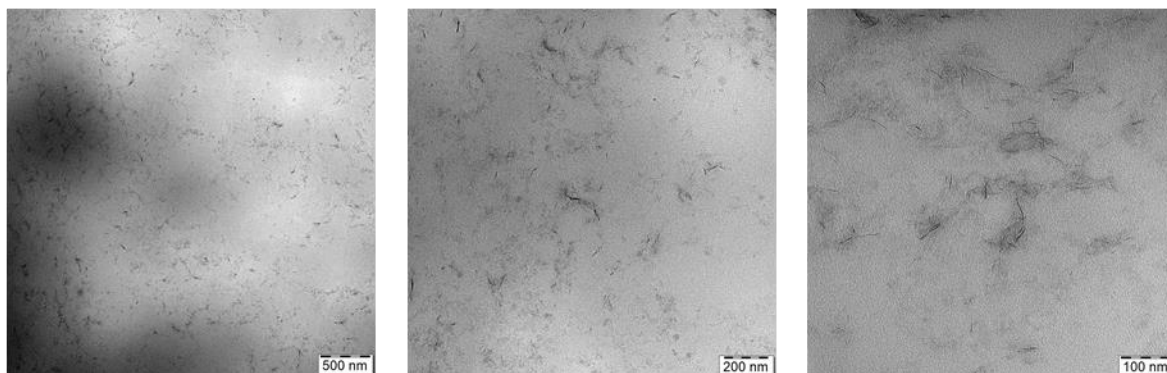
² *Faculty of Chemistry, Rzeszow University of Technology, al. Powstancow Warszawy 6,
PL-35-959 Rzeszow, Poland*

1 Morphology: TEM

2R

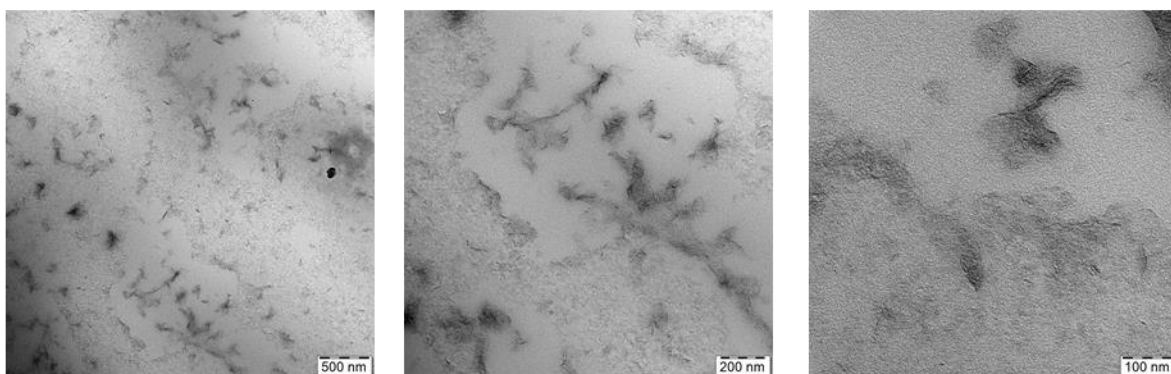


2R-10S

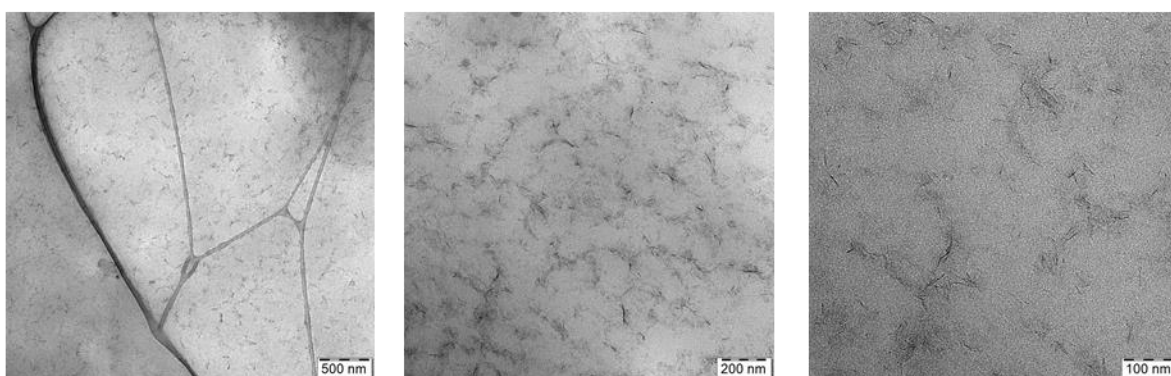


SI-Fig. S1. Morphology of the nanocomposites “2R” (top row) and 2R-10S (bottom row), displayed at different zoom: scalebar: 500 nm (left), 200 nm (centre), and 100 nm (right).

4R

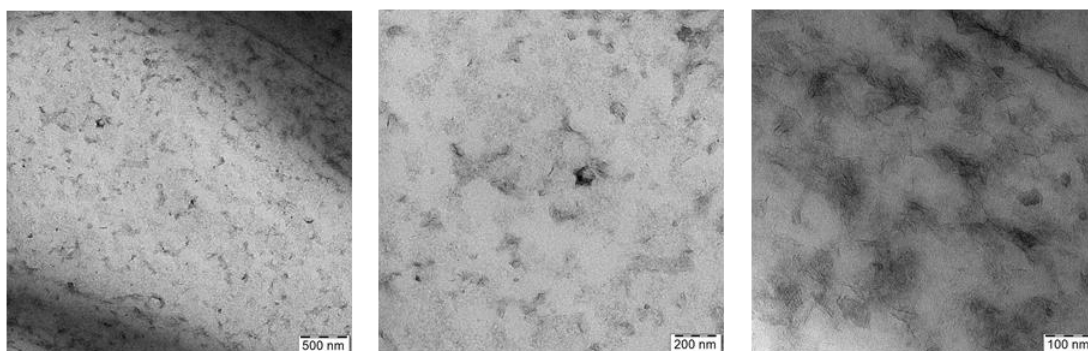


4R-10S



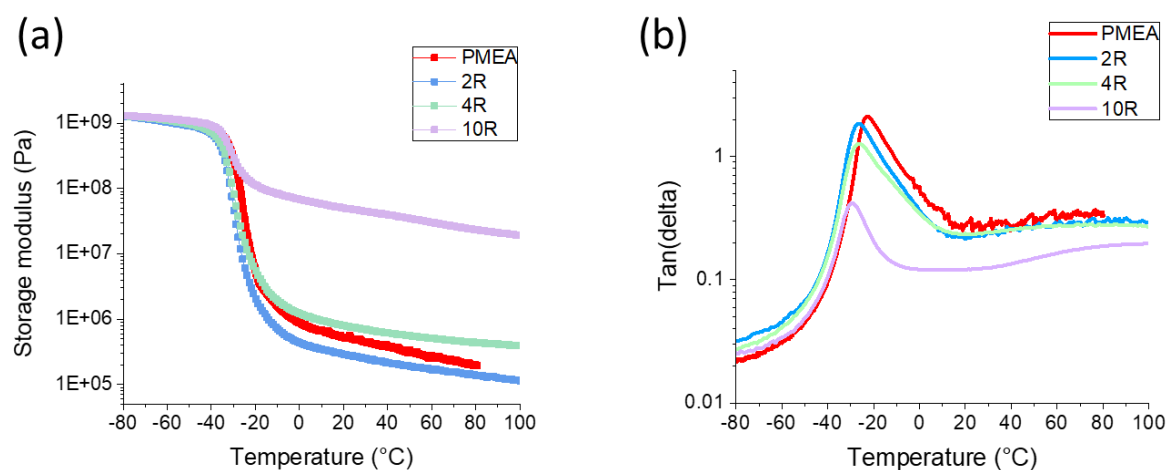
SI-Fig. S2. Morphology of the nanocomposites “4R” (top row) and 4R-10S (bottom row), displayed at different zoom: scalebar: 500 nm (left), 200 nm (centre), and 100 nm (right).

10R

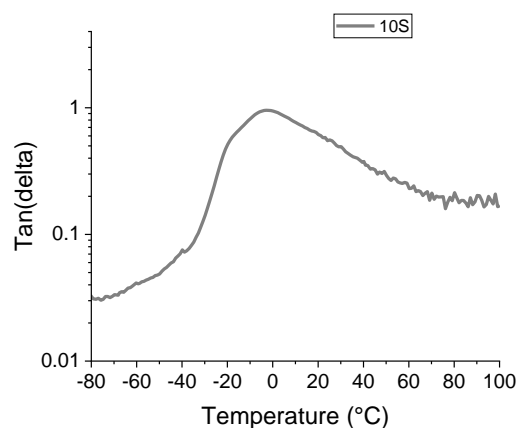


SI-Fig. S3. Morphology of the nanocomposite “10R” displayed at different zoom: scalebar: 500 nm (left), 200 nm (centre), and 100 nm (right).

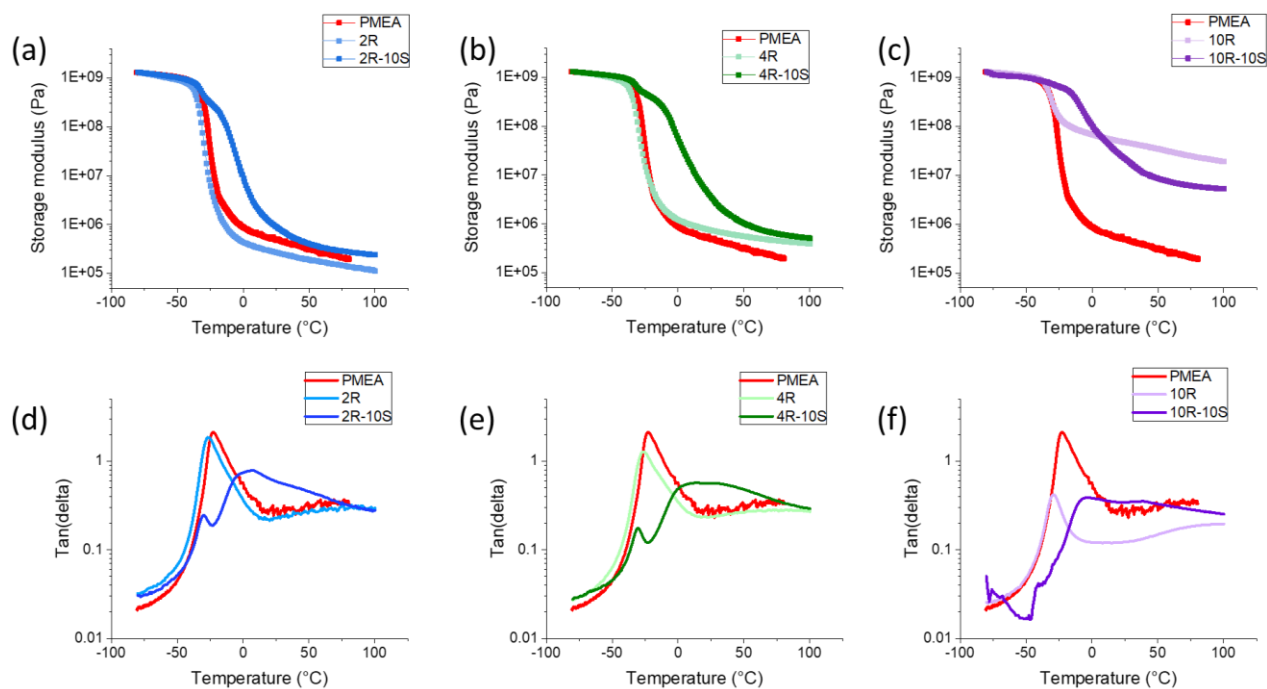
2 DMTA: Thermo-mechanical properties



SI-Fig. S4. Effect of clay (RDS, acting as physical crosslinker) on thermo-mechanical properties: DMTA analysis of neat polyMEA and of nanocomposites with 2, 4, and 10 wt.% of RDS clay (PMEA, 2R, 4R and 10R, respectively): (a) curves of the temperature-dependence of storage shear moduli (G'); (b) curves of the temperature-dependence of the loss factor ($\tan(\delta)$).

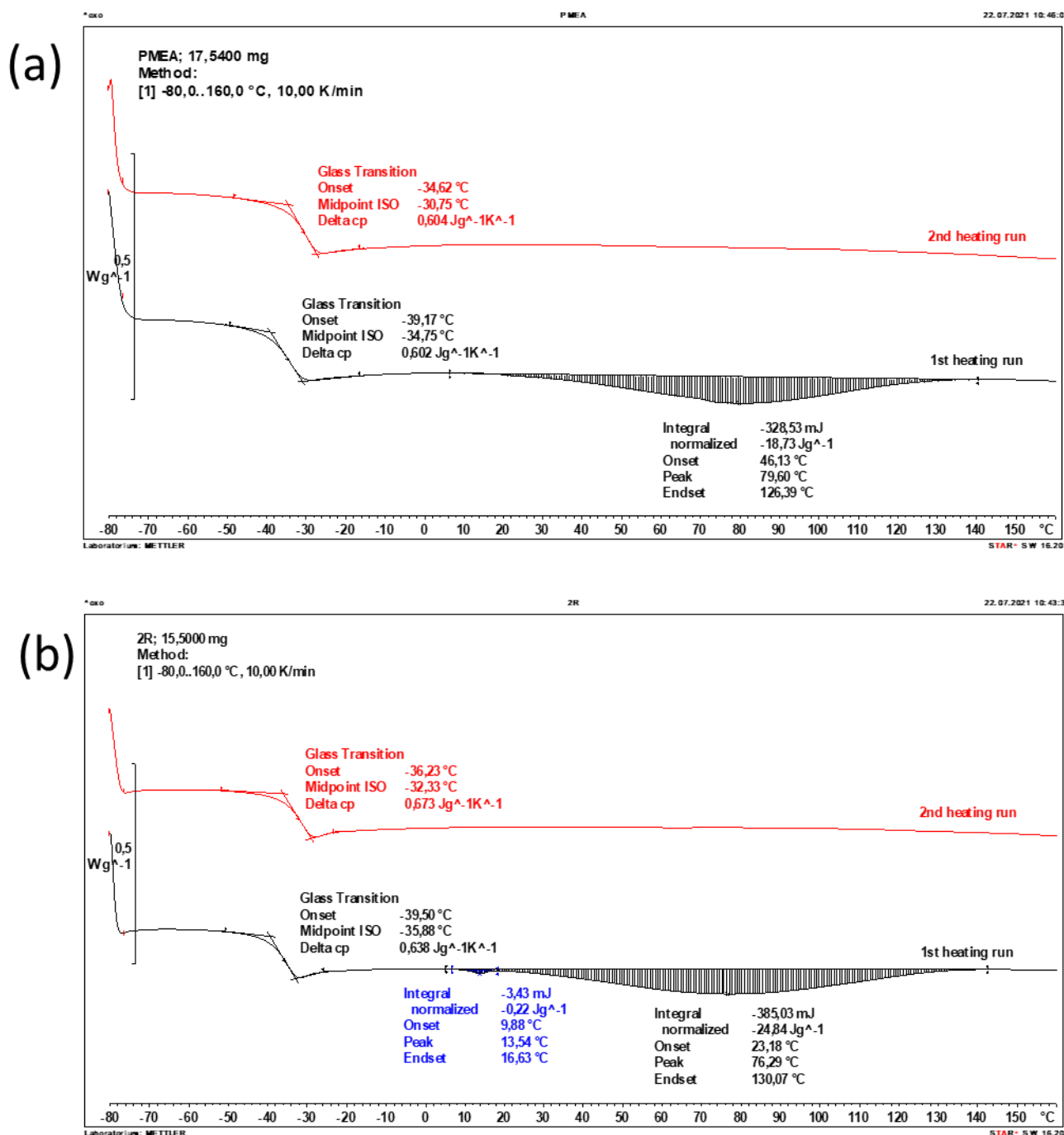


SI-Fig. S5. DMTA analysis of the SMA-free 'linear' co-polymer poly(MEA-co-10mol%SMA): curve of the temperature-dependence of the loss factor $\tan(\delta)$.

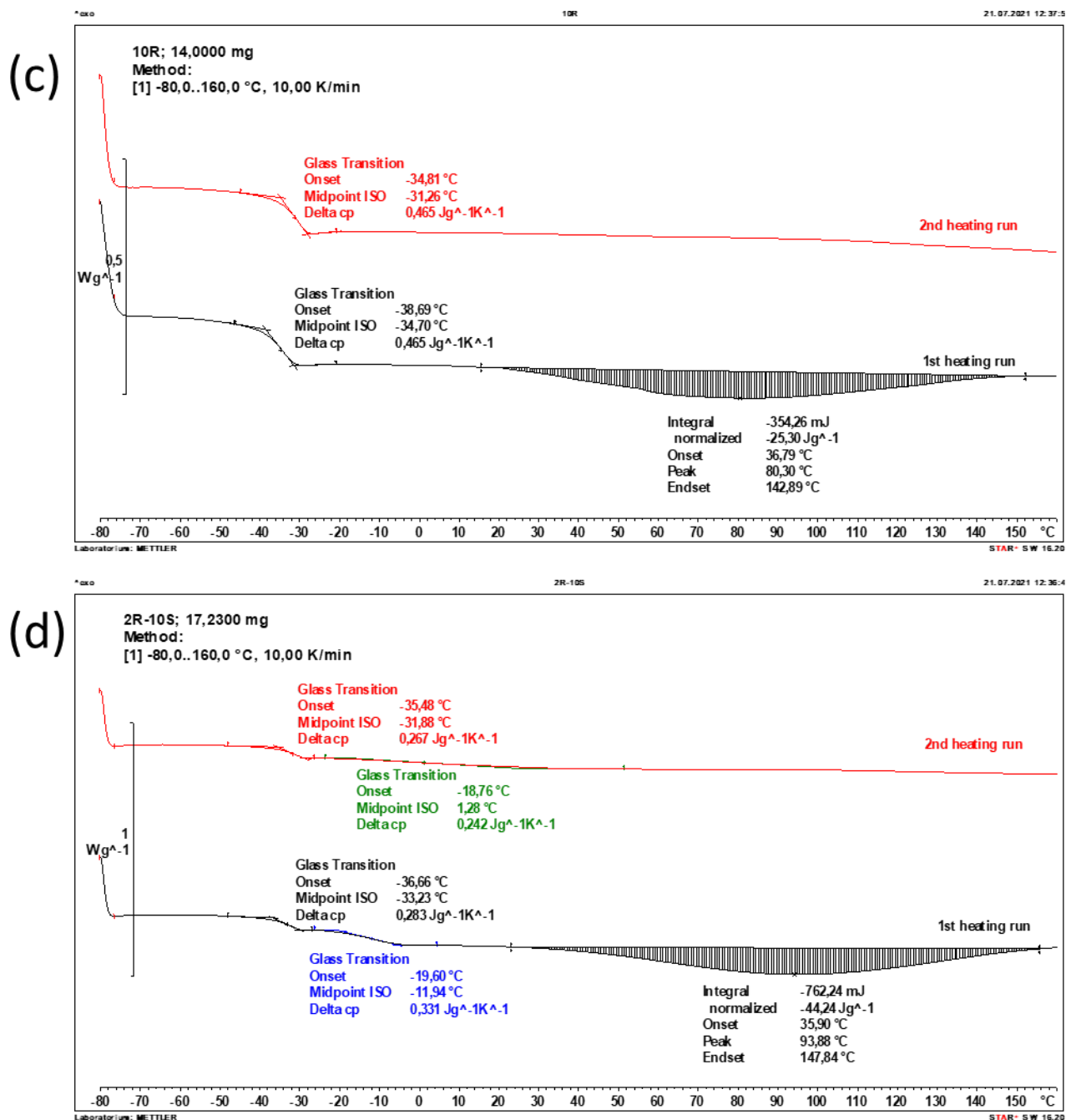


SI-Fig. S6. Dynamic-mechanical thermal analysis (DMTA) of nanocomposites loaded with 2 (a, d), 4 (b, e) and 10 wt.% of clay (c, f): in each graph, the SMA-free composite is compared with its analogue doped by 10 mol% of SMA and with the neat polyMEA matrix; the top row (a – c) compares curves of temperature-dependent storage shear moduli (G'); the bottom (d – f) row compares the curves of the temperature-dependence of the loss factor $\tan(\delta)$.

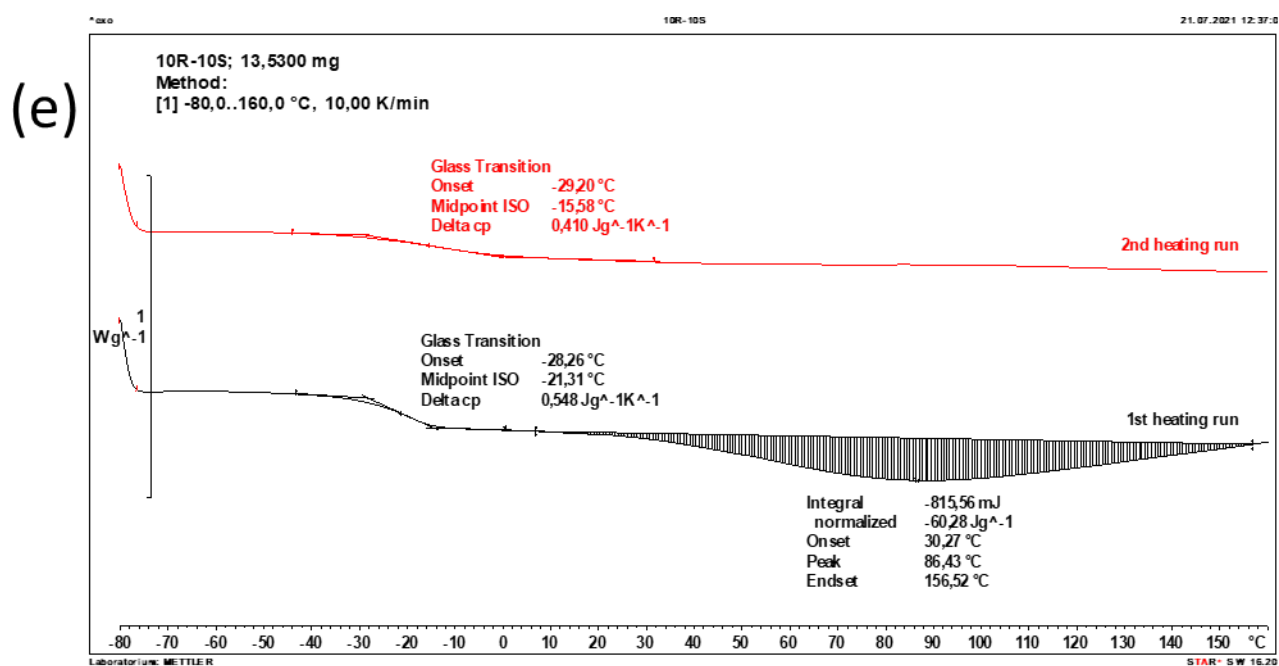
3 DSC: Thermal transitions



SI-Fig. S7. (part 1/3): DSC traces of (a) neat polyMEA; and (b) of the SMA-free nanocomposite 2R, based on polyMEA filled with 2 wt.% of RDS clay.

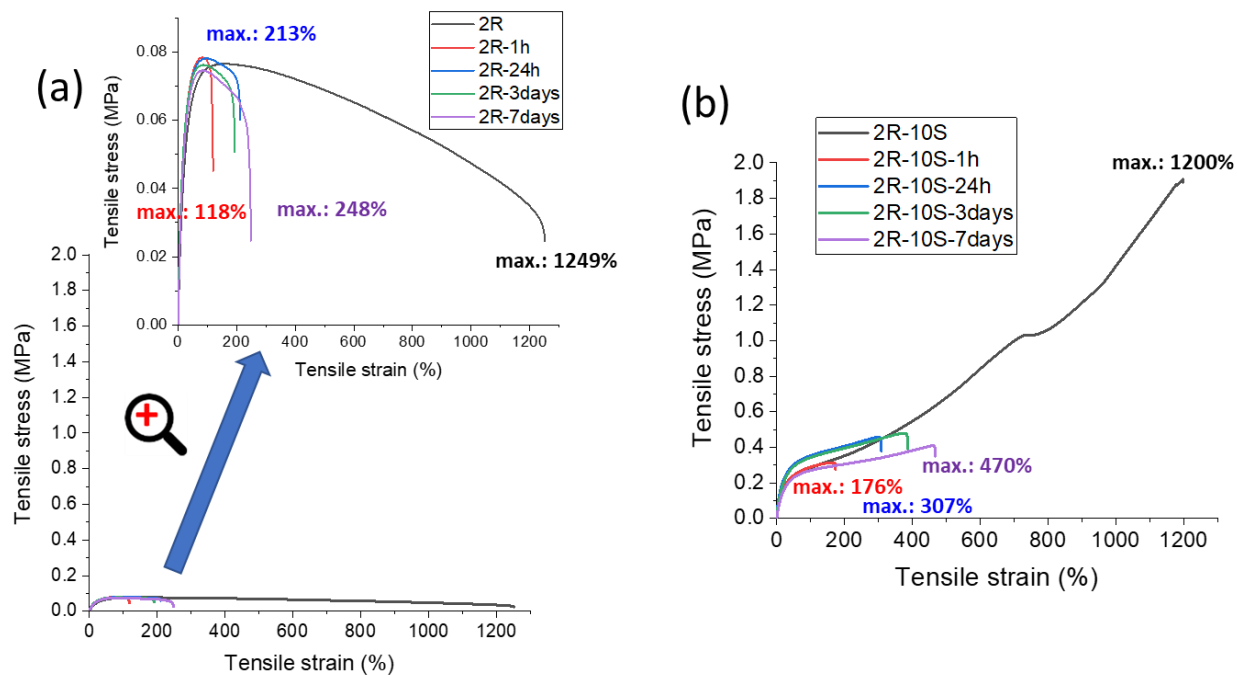


SI-Fig. S7. (part 2/3): DSC traces of (c) the SMA-free nanocomposite 10R, based on polyMEA filled with 10 wt.% of RDS clay; and (d) of the nanocomposite 2R-10S filled with 2% of clay and doped with 10 mol% of SMA.

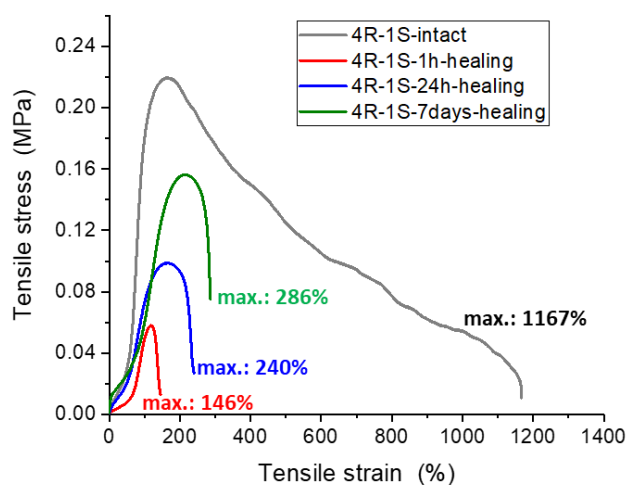


SI-Fig. S7. (part 3/3): DSC trace of (e) the nanocomposite 10R-10S, based on polyMEA filled with 10 wt.% of RDS clay and doped with 10 mol% of SMA.

4 Self-healing of disrupted samples

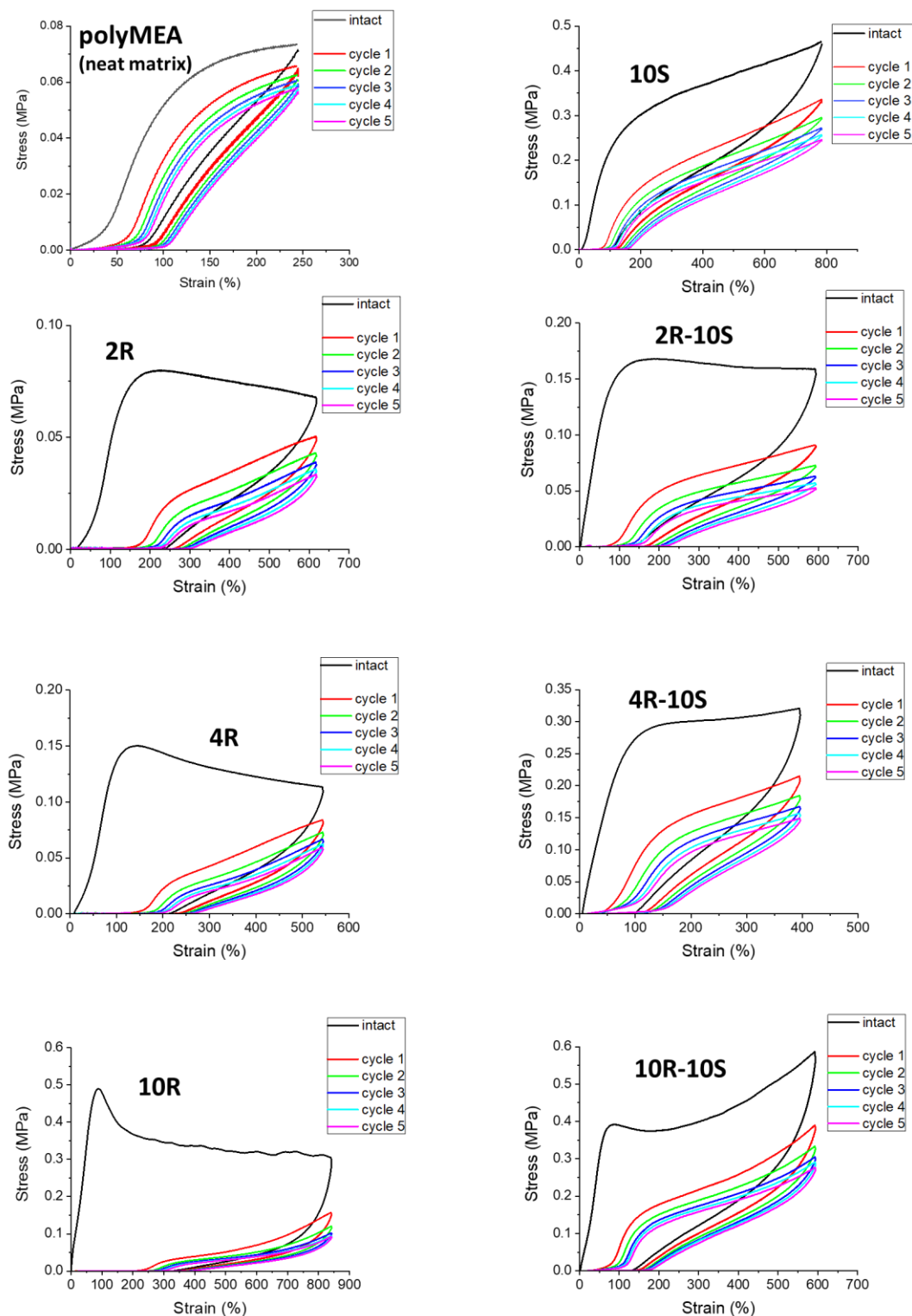


SI-Fig. S8. Self-healing of nanocomposite elastomers based on poly(MEA) crosslinked by 2 wt.% of clay: (a) SMA-free ("2R") and (b) SMA-doped (10 mol%) system ("2R-10S").



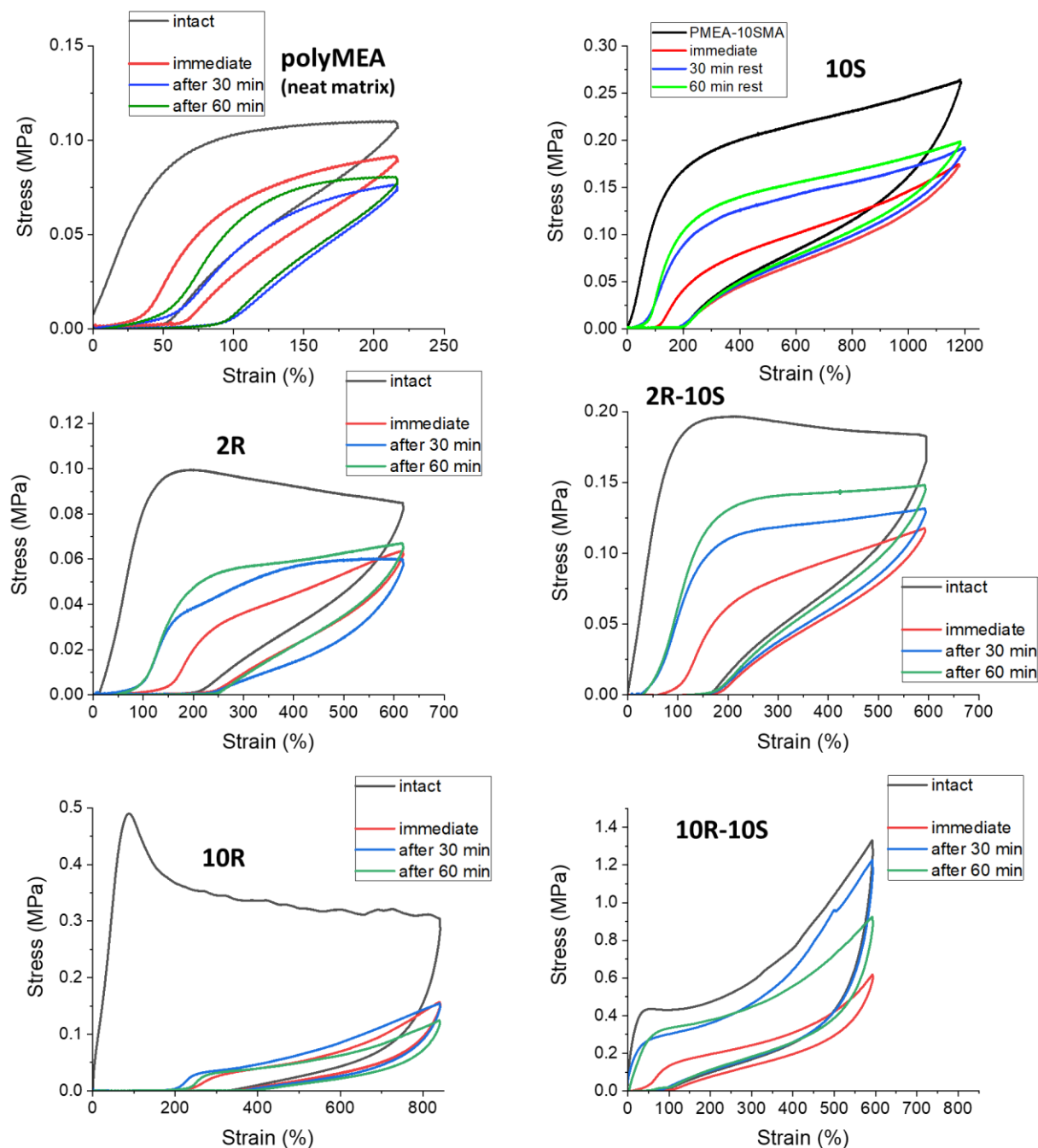
SI-Fig. S9. Self-healing of 4R-1S, a nanocomposite elastomer based on poly(MEA) crosslinked by 4 wt.% of clay and doped by 1 mol% of SMA.

5 Creep vs. elasticity: Cyclic stretching tests



SI-Fig. S10. Repeated cyclic loading test for (left column) the 'linear' polymer (polyMEA) and for the SMA-free nanocomposites 2R, 4R and 10R; and (right column) for their analogues doped by 10 mol% of SMA: 10S (= doped 'linear' polyMEA), 2R-10S, 4R-10S and 10R-10S; the graphs are maximally zoomed and have different X and Y scales; the comparison shows the different nature of response to cyclic loading.

6 Self-recovery: internal self-healing



SI-Fig. S11. Images of self-recovery tests of clay-free samples polyMEA and 10S (= doped 'linear' polyMEA doped with 10 mol% of SMA), of the SMA-free nanocomposites 2R and 10R, and of their SMA-doped analogues 2R-10S and 10R-10S.